

The Cosmic Baryon Fraction and the Extragalactic Ionizing Background

Lam Hui^a, Zoltán Haiman^b, Matias Zaldarriaga^c and Tal Alexander^d

^a Department of Physics, Columbia University, 538 West 120th Street, New York, NY 10027

^b Princeton University Observatory, Princeton, NJ 08544

^c Physics Department, New York University, 4 Washington Place, New York, NY 10003

^d Space Telescope Science Institute, 3700 San Martin Drive, Baltimore, MD 21218

lhui@astro.columbia.edu, zoltan@astro.princeton.edu, matiasz@physics.nyu.edu,
tal@stsci.edu

ABSTRACT

We reassess constraints on the cosmological baryon density from observations of the mean decrement and power spectrum of the Lyman- α forest, taking into account uncertainties in all free parameters in the simplest gravitational instability model. The uncertainty is dominated by that of the photoionizing background, but incomplete knowledge of the thermal state of the intergalactic medium also contributes significantly to the error-budget. While current estimates of the baryon fraction from the forest do prefer values that are somewhat higher than the big bang nucleosynthesis value of $\Omega_b h^2 = 0.02 \pm 0.001$, the discrepancy is at best about 3σ . For instance, assuming the highest estimate of the ionizing background, as indicated by recent measurements of a large escape fraction from Lyman-break galaxies by Steidel, Pettini & Adelberger, we find $\Omega_b h^2 = 0.045 \pm 0.008$. A recent measurement of the ionizing background from the proximity effect by Scott et al., on the other hand, implies $\Omega_b h^2 = 0.03 \pm 0.01$. We provide an expression from which future likelihoods for $\Omega_b h^2$ can be derived as measurements of the ionizing background improve – consistency among constraints from the forest, nucleosynthesis and the microwave background will provide a powerful test of the gravitational instability model for the forest, and for large scale structure in general. We also develop a formalism which treats lower bounds on the baryon density in a statistical manner, which is appropriate if only a lower bound on the ionizing background is known. Finally, we discuss the implications of the escape fraction measurement for the age, structure and stellar content of Lyman-break galaxies.

Subject headings: cosmology: theory – intergalactic medium – large scale structure of universe; quasars – absorption lines

1. Introduction

It has long been recognized that the intergalactic medium (IGM) is highly ionized, and likely contains a substantial fraction of the universe’s baryons at redshifts $z \sim 3$ (e.g. Gunn & Peterson 1965, Steidel & Sargent 1987, Fukugita, Hogan & Peebles 1998 and references therein). Constraints on the baryon density $\Omega_b h^2$ (where Ω_b is a fraction of the critical density, and h is the Hubble constant today in units of 100 km/s/Mpc) from observations of the Lyman- α (Ly α) forest rely on assumptions about the size and geometry of the absorbing structures (see e.g. Rauch & Haehnelt 1995). Recent advance in theoretical modeling of the forest provides a framework in which fluctuations seen in absorption arise naturally out of gravitational instability, and which successfully matches the gross observed properties of the forest (e.g. Bi, Borner & Chu 1992; Cen

et al. 1994; Zhang et al. 1995; Reisenegger & Miralda-Escudé 1995; Hernquist et al. 1996; Miralda-Escudé et al. 1996; Muecket et al. 1996; Bi & Davidsen 1997; Bond & Wadsley 1997; Croft et al. 1998; Hui, Gnedin & Zhang 1997; Thuens et al. 1999; Bryan et al. 1999; Croft et al. 1999; Nusser & Haehnelt 2000; but see also Meiksin, Bryan & Machacek 2001 for possible problems, and Zaldarriaga et al. 2001 for consistency checks). This framework makes definite predictions about the spatial distribution of the absorbing structures, making it possible to obtain useful constraints on $\Omega_b h^2$ from forest observations (e.g. Rauch et al. 1997; Weinberg et al. 1997; McDonald et al. 2000) – once the photoionizing background, which determines the overall neutral fraction, is specified.

Three recent developments motivate us to re-examine the Ly α forest constraints on the cosmological baryon fraction. First, the recent microwave background anisotropy measurements favor a baryon fraction that is higher than the big bang nucleosynthesis value inferred from deuterium measurements (the former gives $0.022 < \Omega_b h^2 < 0.040$, 2- σ limits for a flat scale-invariant inflation model, see de Bernardis et al. 2000; Hanany, S. et al. 2000; Tegmark & Zaldarriaga 2000; Jaffe et al. 2000; Lange et al. 2001; the latter gives 0.02 ± 0.001 , 1- σ error, see Burles, Nollet & Turner 2000; see also Burles & Tytler 1998 for earlier constraints). Second, Steidel, Pettini & Adelberger (2001) reported measurements of a large escape fraction of ionizing photons from Lyman break galaxies (LBG’s) at $z \sim 3$, which imply an extragalactic ionizing flux that is significantly larger than what one might expect from quasars alone. A larger photo-ionizing background implies a smaller neutral fraction, and so a larger baryon density is required to match the given observed mean absorption seen in the forest. Lastly, analysis of the Ly α forest has moved beyond comparisons with a restricted set of cosmological models to a point where several parameters specifying the mass power spectrum and the thermal state of the IGM can be determined at the same time from the data (e.g. Choudhury, Srianand & Padmanabhan 2000, Zaldarriaga, Hui & Tegmark 2000). Since earlier forest constraints on the baryon fraction focused on fixed cosmological models and/or reionization history (and therefore fixed thermal state)¹, it is timely to examine how uncertainties in these parameters impact the estimates for $\Omega_b h^2$. Because the Ly α constraint on the baryon fraction is completely independent of constraints from nucleosynthesis or the microwave background, comparing all three provides a powerful consistency check of the inflation + cold dark matter structure formation model, as well as a test of current ideas about the nature of the forest.

We briefly review in §2.1 the gravitational instability model for the Ly α forest, and how it is used to obtain estimates of the baryon density. Discussions in the literature have focused on two different approaches. One (e.g. Haehnelt et al. 2000) implicitly assumes that most of the universe’s baryons is in the IGM², and that the total ionizing background can be largely accounted for by directly summing up the contributions from known sources, or obtained from indirect measurements of the sum total background, such as those using the proximity effect. The other approach (e.g. Rauch et al. 1997; Weinberg et al. 1997) is more conservative, assuming only a lower limit to the ionizing background from known sources – this gives a lower bound on the neutral fraction and therefore a lower bound for the $\Omega_b h^2$. We will discuss both approaches.

We describe in §2.2.1 how lower bounds given in the literature can be interpreted in a statistical manner, generalizing earlier work where only strict lower bounds are discussed. As we will see, uncertainties in the

¹A notable exception is Weinberg et al. (1997) who attempted to give the most conservative lower bounds on the baryon density. We provide here a statistical framework for interpreting such lower bounds.

²Estimates so far do give values for the baryon density that are close to or even higher than the nucleosynthesis value (e.g. Rauch et al. 1997, McDonald et al 2000). Detailed accounting of the universe’s baryon budget also supports the notion that most of the baryons are in the IGM (Fukugita et al. 1998).

level of the ionizing background dominate uncertainties in the current bound on $\Omega_b h^2$. In §2.2.2, we relate the lower-bound likelihood in §2.2.1 to the (differential) likelihood for baryon density, assuming effectively that most of the universe’s baryons are in the IGM and that the ionization background is known. As we will emphasize in §2.2.2, non-negligible uncertainties in the estimates for $\Omega_b h^2$ remain *even if* the ionizing background is known to high accuracy. This is because of degeneracy with other parameters in the gravitational instability model. We will examine which parameters are the most important in this regard. The likelihood of $\Omega_b h^2$ for a fixed ionizing background is also given (an explicit expression is also presented in §4), which can be used to compute future likelihoods as measurements of the ionizing background improve.

Some of the conclusions in the above sections depend critically on the ionizing flux inferred from observations of Lyman break galaxies (Steidel et al. 2001). The fraction of hydrogen-ionizing photons that escape from these galaxies is significantly higher than what is observed in local galaxies, and what is naively expected in simple theoretical models. In §3, we investigate the type of cold gas distribution that would allow these early galaxies to have a high escape probability for ionizing photons. Finally, we conclude in §4, where the issue of escape fraction from quasars is also discussed.

Some of the issues in this paper have been addressed in two recent works. Haehnelt et al. (2000) used previous bounds to derive new limits on $\Omega_b h^2$, using the Steidel et al. measurement of the escape fraction – the treatment assumed the same cosmological model and reionization history upon which the previous respective bounds were based. They also briefly discussed the significance the Steidel et al. results in the context of population synthesis model spectra, and the escape fraction expected based on the amount of gas inferred from the star-formation rate. Choudhury, Srianand & Padmanabhan (2001) used the lognormal approximation to derive bounds on the ratio of $(\Omega_b h^2)^2$ to the ionizing flux, where the thermal state of the gas is allowed to vary, for a fixed cosmological model. Here, we examine the $\Omega_b h^2$ constraints using N-body simulations for a suite of cosmological models (i.e. varying power spectrum) and thermal histories. We also consider the implication of the high observed escape fraction for the age, structure and stellar content of Lyman-break galaxies in greater detail.

2. Baryon Fraction from the Lyman α Forest

2.1. The Gravitational Instability Model for the Forest

We describe briefly here the Ly α forest model used in this paper. It is largely motivated by the success of numerical simulations in matching the observed properties of quasar absorption spectra (see Cen et al. 1994 and related references in §1). The Ly α optical depth τ along the line of sight is given by $A(1 + \delta)^\alpha$, mapped to redshift space, and smoothed with the thermal broadening window (see e.g. Hui, Gnedin & Zhang 1997 for details). The quantity δ is the baryon overdensity $\delta\rho/\bar{\rho}$. The constant α is given by $2 - 0.7(\gamma - 1)$ where γ is the equation of state index – i.e. the temperature of the gas T is related to density by $T = T_0(1 + \delta)^{\gamma-1}$, where T_0 is the temperature at mean density (Croft et al. 1997, Hui & Gnedin 1997). The constant A is given by (e.g. Weinberg et al. 1997)³

$$A = 0.18 \left[\frac{\Omega_b h^2}{0.02} \right]^2 \left[\frac{1}{J_{\text{HI}}} \right] \left[\frac{T_0}{10^4 \text{ K}} \right]^{-0.7} \left[\frac{0.7}{h} \right] \left[\frac{1+z}{4} \right]^6 \quad (1)$$

³ $A = \bar{n}_{\text{HI}} c H(z)^{-1} \sigma_{\alpha 0}$, where \bar{n}_{HI} is the neutral hydrogen density at $\delta = 0$, c is the speed of light, and $H(z)$ is the Hubble parameter at redshift z , and $\sigma_{\alpha 0} = 4.478 \times 10^{-18} \text{ cm}^2$: the Ly α absorption cross-section is given by $\sigma_{\alpha 0}$ times the Voigt profile.

$$\left[\frac{X_{\text{H}}}{0.76} \right] \left[\frac{X_{\text{H}} + X_{\text{He}}/2}{0.88} \right] \left[\frac{4.461}{\sqrt{\Omega_m(1+z)^3 + \Omega_\Lambda + (1 - \Omega_m - \Omega_\Lambda)(1+z)^2}} \right]$$

where h is the Hubble constant today in units of 100 km/s/Mpc, z is the redshift, X_{H} is the mass fraction of baryons that is in hydrogen, X_{He} is the same for helium, the assumption being that both H and He are highly ionized.⁴ The factor of 4.461 in the last term corresponds to a model with $\Omega_m = 0.3$, $\Omega_\Lambda = 0.7$ and $z = 3$. We have used the recombination rate coefficient $\alpha_{\text{rec.}} = 4.2 \times 10^{-13} (T/10^4 \text{ K})^{-0.7} \text{ cm}^3 \text{ s}^{-1}$ (Rauch et al. 1997).

The dimensionless quantity J_{HI} is defined by

$$\begin{aligned} & J_{\text{HI}} \times 10^{-21} \text{ erg s}^{-1} \text{ cm}^{-2} \text{ Hz}^{-1} \text{ ster}^{-1} \\ &= \int_{\nu_{\text{HI}}}^{\infty} 4\pi j_\nu \sigma_{\text{HI}}(\nu) \frac{d\nu}{\nu} / \int_{\nu_{\text{HI}}}^{\infty} 4\pi \sigma_{\text{HI}}(\nu) \frac{d\nu}{\nu} = j_{\nu_{\text{HI}}} \left[\frac{3}{\beta + 3} \right] \end{aligned} \quad (2)$$

where j_ν is the specific intensity of the ionizing background, $\nu_{\text{HI}} = c/912\text{\AA}$, σ_{HI} is the ionizing cross-section for HI ($\sigma_{\text{HI}}(\nu)$ is approximately $6.3 \times 10^{-18} \text{ cm}^2 (\nu/\nu_{\text{HI}})^{-3}$ for ν just above ν_{HI} ; but see below), and β is the slope of j_ν just above ν_{HI} : $j_\nu \propto \nu^{-\beta}$. The photoionization rate Γ_{HI} is related to J_{HI} by

$$\Gamma_{\text{HI}} = 4.3 \times 10^{-12} J_{\text{HI}} \text{ s}^{-1} \quad (3)$$

The expression here, together with eq. (2) above, gives the correct relationship between $j_{\nu_{\text{HI}}}$ and Γ_{HI} that is accurate to within 3%, for all values of β between 0 and 3. This takes into account slight departure of $\sigma_{\text{HI}}(\nu)$ from an exact ν^{-3} power-law (see Osterbrock 1989, eq. 2.4).

Given a structure formation model such as the Cold Dark Matter (CDM) model, the distribution of δ follows from gravitational instability, and can be predicted using hydrodynamic, N-body (with suitable smoothing) or Hydro-PM (Gnedin & Hui 1998) simulations. Combining the δ fluctuations with the relation for the optical depth $\tau = A(1 + \delta)^\alpha$ (with suitable mapping to redshift space and thermal broadening), one can predict a host of observable properties for the Ly α forest, for any given value of A and α . Two observables that have attracted a lot of attention and have been well measured are the transmission power spectrum and the mean decrement ($1 - \langle e^{-\tau} \rangle$). These measurements can be used to yield constraints on parameters in the model, including A which is proportional to $(\Omega_b h^2)^2$.

In this paper, we make use of the analysis by Zaldarriaga, Hui & Tegmark (2000), who obtained constraints on 6 different parameters by matching the observed transmission power spectrum and mean decrement at $z = 3$ from McDonald et al. (2000). The 6 parameters are the mass power spectrum slope and normalization, the gas temperature at mean density T_0 , the equation of state index γ , the normalization factor A (eq. [1]), and k_f , which is the smoothing scale that defines the smoothing of gas relative to dark matter.⁵ The quantity of interest for our purpose here is the combination $AT_4^{0.7} \equiv A(T_0/10^4 \text{ K})^{0.7}$, which is directly proportional to $(\Omega_b h^2)^2/J_{\text{HI}}$. From the analysis of Zaldarriaga et al. (2000), it is straightforward to obtain the likelihood for $AT_4^{0.7}$, marginalized over the other parameters. This is shown in Fig. 1a. It

⁴Assuming instead that He is only singly ionized, which amounts to changing $2X_{\text{He}}$ to X_{He} , will make little difference given our other sources of uncertainties. Whether helium is singly ionized or not of course has profound implications for the spectrum of the ionizing radiation – that is taken into account by the parameter J_{HI} .

⁵In principle, parameters such as Ω_m and Ω_Λ also affects the predicted forest properties, but at redshift 3, Ω_Λ is negligible and Ω_m is close to unity. The cosmological constant Ω_Λ does affect the translation between velocities and distances – the mass power spectrum slope and normalization are essentially fixed at the relevant velocity scales.

provides the starting point for our analysis below. It is worth mentioning that the mean decrement from McDonald et al. (2000) has not been corrected for a possible bias introduced by continuum-fitting. However, comparing their measurement with that from Rauch et al. (1997), who did attempt a correction (which is model dependent), reveals that the bias is comparable to the error-bar given by McDonald et al., who gives $\langle e^{-\tau} \rangle = 0.684 \pm 0.023$ at $z = 3$.

2.2. Likelihood for the Baryon Fraction

The likelihood for $AT_4^{0.7}$ shown in Fig. 1a can, in principle, be translated directly into a likelihood for $\Omega_b h^2$ after marginalization over other parameters that appear in A (eq. [1]), including J_{HI} , h , etc. However, as mentioned in §1, there are at least two reasons why, strictly speaking, one obtains only lower bounds for the baryon fraction – first, not all baryons are necessarily in the forest, although a large fraction does appear to be (i.e. $\Omega_b h^2$ in eq. [1] refers to only those baryons in the forest); second, one often has strictly speaking only lower limits on the ionizing background J_{HI} , based on summing over contributions from known sources (an exception is the use of the proximity effect; another exception is an observational *upper* limit on J_{HI} from searches for fluorescent Ly α emission; both are discussed below). In this section, we will discuss both the likelihood for $\Omega_b h^2$ – as if all or most baryons are in the forest, and the total J_{HI} is known – as well as the lower-bound-likelihood for $\Omega_b h^2$.

2.2.1. A Probabilistic Analysis of Lower Bounds

Let us begin by developing the idea of a lower-bound-likelihood. Previous work often gave lower bounds on the baryon fraction as if they were strict bounds. Of course, uncertainties in J_{HI} , in the measured mean decrement, and in other parameters such as T_0 imply that such bounds have to be given a probabilistic interpretation. We show here the proper quantity to consider is *a lower limit on the probability that $\Omega_b h^2$ is larger than some value*.

We have from eq. (1) $\Omega_b h^2 = \sqrt{AT_4^{0.7} J_{\text{HI}} f(q)}$, where q represents the parameters $h, \Omega_m, \Omega_\Lambda$, and $f(q)$ is some function which can be read off from eq. (1) (we will focus on $z = 3$ in this paper). The probability that $\Omega_b h^2$ is larger than some value B_0 is given by

$$\begin{aligned}
 & \int_{B_0}^{\infty} P(\Omega_b h^2) d(\Omega_b h^2) \\
 &= \int dq d(AT_4^{0.7}) P(q) P(AT_4^{0.7}) \int_{B_0^2/AT_4^{0.7}f(q)}^{\infty} P_{\text{all}}(J_{\text{HI}}) dJ_{\text{HI}} \\
 &\geq \int dq d(AT_4^{0.7}) P(q) P(AT_4^{0.7}) \int_{B_0^2/AT_4^{0.7}f(q)}^{\infty} P(J_{\text{HI}}) dJ_{\text{HI}} \\
 &\equiv P_{>}(\Omega_b h^2 > B_0)
 \end{aligned} \tag{4}$$

where $P(q), P(AT_4^{0.7}), P(J_{\text{HI}})$ represent the probability distributions of $q, AT_4^{0.7}$ and J_{HI} . We use $P_{\text{all}}(J_{\text{HI}})$ to denote the probability distribution for the ionizing intensity from *all* possible sources, while the probability distribution $P(J_{\text{HI}})$ that we will use, at least for some of the calculations below, comes from a summation over contributions from *known* sources, including Lyman-break galaxies and quasars. The inequality above can be understood as follows. For any random variable $Z = X + Y$ with $X, Y \geq 0$ and independent, we have $\int_{Z_0}^{\infty} P_Z(Z) dZ = \int_0^{\infty} dY P_Y(Y) \int_{Z_0-Y}^{\infty} dX P_X(X) \geq \int_0^{\infty} dY P_Y(Y) \int_{Z_0}^{\infty} dX P_X(X) = \int_{Z_0}^{\infty} dX P_X(X)$. By the

same reasoning, the fact that the amount of baryons in the forest is necessarily smaller than the cosmological total only serves to strengthen the inequality in eq. (4). We introduce the symbol $P_{>}(\Omega_b h^2 > B_0)$ to denote the lower limit to the cumulative probability that $\Omega_b h^2$ is larger than some value B_0 .

There are therefore, three probability distributions that we have to specify: $P(AT_4^{0.7})$ is already given in Fig. 1a – that is the input from observations of the Ly α forest; $P(q)$ does not actually affect our conclusions very much, but we will assume a flat universe, with independent Gaussians for $\Omega_m h$ (0.28 ± 0.09 ; Eisenstein & Zaldarriaga 2001) and h (0.72 ± 0.08 ; Freedman et al. 2001) (at $z = 3$, Ω_Λ plays essentially no role); $P(J_{\text{HI}})$ is what we turn to next. There are three main sources of information.

A recent analysis of proximity effect by Scott et al. (2000) (see also Giallongo et al. 1996, Cooke, Epsey & Carswell 1997) gave $\Gamma_{\text{HI}} = 1.9_{-1.0}^{+1.2} \times 10^{-12} \text{ s}^{-1}$, averaged from $z = 1.7$ to 3.8, which translates into $J_{\text{HI}} = 0.44_{-0.23}^{+0.28} \text{ s}^{-1}$. This is presumably the ionizing background from all possible sources.

Steidel et al. (2001) gave $j_{\nu_{\text{HI}}} = 1.2 \pm 0.3 \times 10^{-21} \text{ erg s}^{-1} \text{ cm}^{-2} \text{ Hz}^{-1} \text{ sr}^{-1}$ from the Lyman-break galaxies (LBG's) at $z \sim 3$.⁶ This is obtained by examining the spectra of those LBG's that are in the bluest quartile of observed LBG UV colors. As pointed out by Steidel et al. (2001), a conservative interpretation would therefore be that no ionizing radiation escapes from the other galaxies, in which case $j_{\nu_{\text{HI}}}$ would be a factor of 4 smaller: $j_{\nu_{\text{HI}}} = 0.3 \pm 0.075 \times 10^{-21} \text{ erg s}^{-1} \text{ cm}^{-2} \text{ Hz}^{-1} \text{ sr}^{-1}$. There are in addition a number of uncertainties, including uncertainty in the mean absorption by the intergalactic medium, and the use of the luminosity function down to magnitudes that are fainter than those used for the escape fraction measurements (see Steidel et al. for details). These uncertainties are smaller than the factor of 4 uncertainty in interpretation. To convert the above into J_{HI} , we use $\beta = 1.4$ (see eq. [2]; we will discuss the reason for this choice of β in §3.1).

Finally, there is the contribution from quasars. Rauch et al. (1997) discussed the various measurements and calculations in some detail, and they arrived at a conservative lower limit of $\Gamma_{\text{HI}} > 7 \times 10^{-13} \text{ s}^{-1}$ ($J_{\text{HI}} > 0.16$) at $z = 2 - 3$, when they consider only known quasars with no extrapolation to the faint end of the luminosity function. We will treat this as a strict lower limit for J_{HI} .⁷

We will work out the lower-bound likelihood in eq. (4) for three different $P(J_{\text{HI}})$'s:

- 1. J_{HI} from the proximity effect;
- 2. J_{HI} from summing the high value of $j_{\nu_{\text{HI}}}$ ($j_{\nu_{\text{HI}}} = 1.2 \pm 0.3 \times 10^{-21}$) from LBG's and Rauch et al.'s value from quasars;
- 3. J_{HI} from summing the low value of $j_{\nu_{\text{HI}}}$ ($j_{\nu_{\text{HI}}} = 0.3 \pm 0.075 \times 10^{-21}$) from LBG's and Rauch et al.'s value from quasars.

The corresponding quoted error-bars are used in setting the probability distributions for J_{HI} . In all cases, quantities that are by definition positive, e.g. J_{HI} , $\Omega_m h$, etc, are constrained to be so.

⁶The quoted number was computed by Steidel et al. assuming Einstein de-Sitter cosmology, but the value is in fact strictly independent of cosmology.

⁷In other words, the probability distribution of J_{HI} from *all* quasars $P_{\text{all q.}}(J_{\text{HI}})$ is assumed to satisfy the inequality $\int_{J_{\text{HI}}^0}^{\infty} P_{\text{all q.}}(J_{\text{HI}}) dJ_{\text{HI}} \geq \int_{J_{\text{HI}}^0}^{\infty} P_{\text{known q.}}(J_{\text{HI}}) dJ_{\text{HI}}$, where J_{HI}^0 can take any given value, and $P_{\text{known q.}}(J_{\text{HI}})$ is the probability distribution of J_{HI} from *known* quasars, and is modeled as a delta function which peaks at $J_{\text{HI}} = 0.175$.

We show in Fig. 1b the result of combining the likelihoods for $AT_4^{0.7}$, q and J_{HI} as described above using eq. (4). To reiterate, the main observational inputs are measurements of the mean decrement and transmission power spectrum of the Ly α forest at $z = 3$. The y-axis is the lower limit to the likelihood that $\Omega_b h^2$ is larger than some value B_0 , $P_{>}(\Omega_b h^2 > B_0)$ as defined in eq. (4). The current big bang nucleosynthesis value inferred from deuterium measurements is $\Omega_b h^2 = 0.02 \pm 0.001$ (Burles, Nollett, Turner 2000). This is ruled out at 79%, 99.8% and 96% (or better) for the choices 1, 2 and 3 above for $P(J_{\text{HI}})$.

The large difference between the curves in Fig. 1b illustrates that the dominant uncertainty by far is that due to J_{HI} . We emphasize, however, even assuming the highest J_{HI} (model 2), the nucleosynthesis value is not strongly excluded by Ly α forest measurements, although there is an inconsistency at the $\sim 3\sigma$ level.

2.2.2. Further Investigations of the Baryon Likelihood

It is instructive to show a different version of Fig. 1b, namely the derivatives of those same curves (with a negative sign) i.e. $-dP_{>}(\Omega_b h^2 > B_0)/dB_0$. This is done in Fig. 2a, whose y-axis now represents the differential probability distributions for $\Omega_b h^2$ ($P(\Omega_b h^2)$, rather than $P_{>}(\Omega_b h^2 > B_0)$; see eq. [4]), *if* one assumes that the majority of the baryons is in the forest, and that the probability distributions for J_{HI} used above actually approximate the true distributions for the *total* J_{HI} . Phrased in this way, the mean values with dispersions for $\Omega_b h^2$ are 0.03 ± 0.01 , 0.045 ± 0.008 and 0.028 ± 0.005 respectively for the choices 1,2 and 3 for $P(J_{\text{HI}})$ laid out previously.

The above represents another way of saying that the present measurements have a weak preference for $\Omega_b h^2$ somewhat larger than the nucleosynthesis value. The error-bars at the moment are dominated by uncertainties in J_{HI} . However, it would be useful to derive a likelihood for $\Omega_b h^2$ assuming J_{HI} is exactly known. Future improvements in measurements of J_{HI} can then be directly translated into improved distributions for $\Omega_b h^2$. To be concrete, we would like to compute $P_*(B'_0)$:

$$P_*(B'_0) \equiv P(\Omega_b h^2 = B'_0, J_{\text{HI}} = 1) = \int dq \frac{2B'_0}{f(q)} P(q) P(AT_4^{0.7} = B'_0{}^2 / f(q)) \quad (5)$$

which is obtained from eq. (4) by setting $P(J_{\text{HI}}) = \delta(J_{\text{HI}} - 1)$. We show $P_*(B'_0 = \Omega_b h^2)$ in Fig. 2b. It is well-approximated by a Gaussian with a mean of 0.046 and a dispersion of 0.0061. This is the likelihood for $\Omega_b h^2$ if J_{HI} were exactly unity. If J_{HI} were 0.5 for instance, then the likelihood for $\Omega_b h^2$ would be a Gaussian with a mean of $\sqrt{0.5} \times 0.046 = 0.033$ and a dispersion of $\sqrt{0.5} \times 0.0061 = 0.0043$. More generally, given any $P(J_{\text{HI}})$, the differential probability distribution for $\Omega_b h^2$ can be easily computed using P_* :

$$P(\Omega_b h^2) = \int \frac{1}{\sqrt{J_{\text{HI}}}} P_*(B'_0 = \Omega_b h^2 / \sqrt{J_{\text{HI}}}) P(J_{\text{HI}}) dJ_{\text{HI}} \quad (6)$$

Or, more rigorously, in cases where $P(J_{\text{HI}})$ accounts for only contributions from known but not all possible sources, and keeping in mind that not all baryons are necessarily in the forest, one can obtain (by integrating eq. [6]) a lower bound on the cumulative probability that $\Omega_b h^2$ is larger than some value – i.e. use $\int_{B_0}^{\infty} P(\Omega_b h^2) d(\Omega_b h^2)$ to obtain $P_{>}(\Omega_b h^2 > B_0)$, just as we have done in §2.2.1.

Fig. 2b illustrates another important point: substantial uncertainties in $\Omega_b h^2$ remain even if J_{HI} were known at high accuracy. The uncertainties can be traced back to the spread in $AT_4^{0.7}$, shown in Fig. 1a. Checking each of the parameters that were marginalized in obtaining $P(AT_4^{0.7})$, we find that the main sources of errors are, in order of importance, T_0 the temperature at mean density, γ the equation of state index, and k_f the smoothing scale of the gas distribution – fixing each of these parameters individually

would decrease the variance in $AT_4^{0.7}$ by 43%, 39% and 31% respectively. Interestingly, fixing the power spectrum normalization and/or slope, or the mean transmission value ($1 - \text{mean decrement}$) decreases the variance of $AT_4^{0.7}$ by no more than 11%. The latter in particular implies that the current accuracy of the mean transmission/decrement measurements at $z \sim 3$ is not the main limiting factor for the accuracy of the $\Omega_b h^2$ constraint; one caveat is that systematic errors such as those due to continuum-fitting might have been underestimated – this is an important question which deserves closer study. In addition to better measurements of J_{HI} , future improvements in constraints on $\Omega_b h^2$ from the Ly α forest will rely on more accurate knowledge of the thermal state of the IGM.

3. The Ionizing Continuum of Lyman Break Galaxies

The most stringent lower limit on $\Omega_b h^2$ (dashed curve in Fig. 1a) depends sensitively on the ionizing continuum ($E > 13.6\text{eV}$) emitted by high-redshift galaxies. This is obtained from the observed composite spectrum of 29 Lyman break galaxies at $z \sim 3.4$ (Steidel et al. 2001).⁸ Because of the importance of the ionizing continuum in determining the likelihood for $\Omega_b h^2$, we discuss here the results of Steidel et al. (2001) in some more detail. In particular, the continuum flux in the Steidel et al. (2001) sample is unexpectedly high (compared with both naive theoretical expectations, and observations of galaxies at low redshifts; see below), and, taken at face value, presents two distinct puzzles: (i) a significant fraction of the ionizing radiation appears to escape from the LBGs, whereas a small escape fraction is expected; and (ii) even assuming that no ionizing photons were lost in escaping from the galaxies, the stellar populations of the LBGs appear to produce a very hard ionizing continuum compared to spectral synthesis models. We address these two issues below, first (ii), and then (i).

3.1. The Ionizing Flux Produced in Lyman Break Galaxies

We first compare the stacked composite spectrum of LBGs in Steidel et al. (2001) with model galactic spectra. We utilize the spectral synthesis models of Leitherer et al. (1999); although we obtained similar conclusions using the models of Bruzual & Charlot (1996). We adopt the stellar models for a Salpeter IMF (with a slope $\alpha = 2.35$) between $1 - 100M_\odot$, metallicity of $Z = 0.4Z_\odot$, and compute the spectrum either for continuous star formation for 10^8 yr, or at the age of 10^6 yr following an instantaneous starburst. These correspond to the models shown in Figures 8d and 7d of Leitherer et al. (1999), respectively. In addition, to simulate the observed composite spectrum, we modify the emitted stellar template spectrum by including the effects of dust absorption, as well as the opacity of the intervening IGM. To include dust opacity, we use the absorption cross-sections for a mix of graphite and silicate grains that reproduces the Milky Way opacities (Draine & Lee 1984), and adjust the total amount of dust by fitting the slope of the observed spectrum at (emitted) wavelengths $\lambda > 1215\text{\AA}$.

In order to assess the intrinsic level of the flux below 912\AA , it is important to model the opacity of the intervening IGM accurately. This opacity is due to Lyman α absorption systems along the lines of sights to the galaxies. We model here the IGM absorption by summing the optical depths of all Lyman α absorbers in

⁸The Steidel et al. measurements strictly speaking constrain J_{HI} at $z \sim 3.4$ rather than 3, as we have used in §2.2. Within the present uncertainties, J_{HI} does not appear to evolve significantly with redshift around $z \sim 3$ (see e.g. Giallongo et al. 1996, Cooke et al. 1997, Scott et al. 2000). We choose to focus on $z = 3$ partly because some of the best existing measurements on mean decrement and transmission power spectrum are at $z = 3$.

the range of neutral HI column densities $10^{12} - 10^{20} \text{ cm}^{-2}$ (see Madau 1995 for a description of the method, and Fardal, Giroux & Shull 1998 for a more recent parameterization of the column density distribution of absorbers). Note that the opacity at wavelengths shorter than 912\AA is dominated by the poorly-known abundance of high-column density absorbers ($N_{\text{HI}} \gtrsim 10^{17} \text{ cm}^{-2}$). However, the relevant integrated quantity that determines the break in the spectrum at 912\AA is better constrained. Using a quasar sample, Steidel et al. (2001) measured the value of the intrinsic ratio of the decrements at 900\AA and 1100\AA , which they find to be a factor of 2.5. In order to match this decrement ratio, and to simultaneously predict a Ly α decrement of $D_A \approx 0.45$ (which we obtained directly from the $z = 3.4$ LBG sample), we found that we had to adopt a column-density distribution intermediate between models A1 and A4 of Fardal et al. (1998).

In Fig. 3, we show the resulting model spectra, superimposed on the composite spectrum of Steidel et al. (2001). The dotted and dashed curves correspond to the models of continuous star formation for 10^8 years, and to the 10^6 yr old starburst, respectively; the solid curves show the data. All fluxes are normalized to the same flux at the emitted wavelength of 1500\AA . In the bottom panel, we also show the optical depths we assumed for the dust and the IGM, respectively (in the continuous star formation case; a somewhat larger dust opacity was needed for the instantaneous starburst). In the top panel, the horizontal dashed line shows the mean observed flux in the wavelength range $880\text{\AA} \leq \lambda \leq 910\text{\AA}$.

As the top panel in Fig. 3 shows, in the $880\text{\AA} \leq \lambda \leq 910\text{\AA}$ range, the mean observed flux is $F_\nu/F_{1500} = 0.06 \pm 0.01$; while the continuous star formation models predict $F_\nu/F_{1500} = 0.027 \pm 0.003$. Taken at face value, the data reveals twice as high an ionizing flux as these models predict, even if we do not include any absorption by cold gas in the galaxy. The starburst model can come close to producing the observed ionizing flux at 912\AA , but only if an age of $\lesssim 10^6$ yr is assumed. Although the 29 galaxies included in the composite spectrum were selected from the bluest quartile of the sample, it appears unlikely that they were typically “caught” at such a young age. A short lifetime does appear to be consistent with the number density and clustering properties of LBG’s (e.g. Wechsler et al. 2001; but see also Mo, Mao & White 1999), but it is disfavored by other arguments, such as the optical to near-infrared colors (Shapley et al., in preparation), and by tentative measurements of mass-to-light ratios (Pettini et al. 2001). The ionizing radiation in the models is dominated by massive OB stars, and, as a result, after $\sim 4 \times 10^6$ years, the starburst model predicts a rapidly diminishing value for the flux below 912\AA .

The starburst model gives a (cross-section weighted) spectral slope of $\beta = 1.4$ below 912\AA ($j_\nu \propto \nu^{-\beta}$). This slope is somewhat harder than typical quasar spectra in the relevant wavelength range just below 912\AA . This is what we have used in §2.2 to convert measurements of $j_{\nu_{\text{HI}}}$ to J_{HI} . The true value for β is likely to be smaller due to absorption by the intergalactic medium – this gives us a lower limit on J_{HI} ($J_{\text{HI}} \propto 1/(\beta + 3)$; see eq. [2]).

Taking the data at face value, the implication is that the stellar populations in LBGs produce \gtrsim twice as many H-ionizing photons as the current models predict. This discrepancy is more severe at shorter wavelengths, where the IGM is expected to become increasingly more opaque. Note that although the mean IGM opacity is directly measured by Steidel et al. at $\lambda \approx 900\text{\AA}$, the variation of the opacity with wavelength across the range $880 - 910\text{\AA}$ depends on the column density distribution of Lyman α absorption systems with column densities $N_{\text{HI}} \gtrsim 10^{17} \text{ cm}^{-2}$, and is more uncertain.

Changing the assumed metallicities, or adding the emission from the nebular continuum, does not significantly increase the predicted ionizing fluxes. The UV fluxes of OB stars can be increased by the presence of stellar winds (not included in the stellar models we adopted). Although winds can increase the HeII-ionizing flux by orders of magnitude, the corresponding increase for the H-ionizing flux in O stars

has been found to be small (Schaerer & de Koter 1997). The increase can be more significant for cooler B–stars (Najarro et al. 1996), but these stars do not dominate the ionizing photon budget in the continuous star–formation models, in which O–stars are continuously replenished. Furthermore, the hydrostatic stellar models typically reproduce the properties of Galactic HII regions (Leitherer et al. 1999), so that an increase by the required factor of ~ 2 would make it more difficult to reconcile the models with these observations.

In summary, we conclude that the stellar population in the galaxies comprising the Steidel et al. (2001) sample appear to be significantly different from spectral synthesis model predictions, and from stellar populations in nearby galaxies, unless the selection procedure somehow strongly favors very young galaxies (i.e. age $\lesssim 10^6$ years). It remains to be seen whether stellar models that include winds can account for the apparent difference. An alternative explanation of the large ionizing flux could be that the IMF at $z \sim 3$ is biased towards massive stars.

3.2. The Escape Fraction of Ionizing Photons From Lyman Break Galaxies

Although the nature of LBGs is not well understood, based on their observed fluxes and clustering properties, they appear to have luminosities similar to $\sim L^*$ galaxies, and to be associated with halos of total mass $\gtrsim 10^{11}M_\odot$ (in most models, see, e.g. Wechsler et al. 2001, and references therein). The escape of ionizing radiation from “normal” disk galaxies has been studied extensively in observations of the Milky Way (Reynolds et al. 1995) and other nearby galaxies (e.g. Leitherer et al. 1995; Hoopes, Walterbos & Rand 1999); as well as theoretically (e.g. Dove & Shull 1994; Dove, Shull & Ferrara 2000). Both theory and observations indicate small escape fractions that are of order $\sim 10\%$. In a theoretical study extending galactic disk models to high redshift, Wood & Loeb (2000) showed that if a few percent of the total gas mass would cool and settle into a rotationally supported thin disk, the escape fraction would be negligible from galaxies at $z \sim 3$ in halos with a total mass $M \gtrsim 10^{11}M_\odot$ (the decrease in f_{esc} being due to the higher densities [$\propto (1+z)^3$] at higher redshifts). In comparison, the escape fraction in the Steidel et al. sample is $f_{\text{esc}} \gtrsim 0.5$.⁹

Ionizing radiation could escape more efficiently from LBGs if most of the cold gas ($T \sim 10^4$ K) were spread over an extended region, rather than incorporated into a fully–formed, dense galactic disk. Such a spatially extended distribution for the cold gas would be natural during the earliest phases of galaxy formation, when galaxy–sized dark halos are assembling for the first time. Alternatively, if star formation in LBGs is triggered by mergers (see this model in Wechsler et al. 2000), then the merger could spread the cold gas over a large solid angle. In either case, the diluted density would reduce the recombination rate ($\propto \rho^2$), making it easier to keep the cold gas photoionized, and for the ionizing radiation to escape.

To quantify the required ionizing photon rate, we consider the simplified toy model for the cold gas distribution described in Haiman & Rees (2001). In this model, the gas initially has a spherically symmetric distribution, with a radial profile dictated by hydrostatic equilibrium in an NFW (Navarro, Frenk & White 1997) dark matter halo. Subsequently, a fraction of the gas, determined by the cooling efficiency, cools to 10^4K , and resides in cold clumps whose densities are compressed by a factor $\sim T_{\text{vir}}/10^4\text{K}$ (where $T_{\text{vir}} \sim 10^6\text{K}$ is the virial temperature of the halo). The rest of the gas remains in the collisionally ionized hot phase, at

⁹Steidel et al. define f_{esc} as the fraction of 900\AA photons that escape the galaxy, divided by the same fraction for 1500\AA photons. Thus, the actual escape fraction of 900\AA photons from the LBGs can be as small as $\sim 15\%$, if dust absorbs $\sim 85\%$ of photons at both wavelengths. Since dust opacity is not included in the theoretical models, this is a fair comparison.

the temperature of T_{vir} .

As an example of this model, the gas in a $10^{12}M_{\odot}$ halo at $z = 3.4$ (virial temperature of $T_{\text{vir}} = 2 \times 10^6\text{K}$, a 2.3σ object) cools out to approximately half of the virial radius ($R_{\text{vir}} \approx 50\text{kpc}$). The total recombination rate within the halo is $R = 4\pi \int_0^{R_{\text{vir}}} r^2 dr f_V n_{\text{H}}(r)^2 \alpha_B$ is $\approx 2 \times 10^{55}\text{s}^{-1}$, where f_V is the volume filling fraction of cold gas (approximately unity out to $R_{\text{vir}}/2$, and dropping to negligible values at larger radii), and α_B is the case-B hydrogen recombination coefficient evaluated at $\approx 10^4\text{K}$. With the standard Salpeter IMF, every stellar proton yields ~ 4000 ionizing photons, so that a star formation rate of $1 M_{\odot} \text{ yr}^{-1}$ translates to a production rate $1.5 \times 10^{53} \text{ s}^{-1}$ of ionizing photons. In order to allow a large escape fraction, most of this cold gas has to be kept photo-ionized. Increasing the above photon production rate by a factor of four, as suggested by the composite spectrum of Steidel et al. (2001), we find that the required “characteristic” star formation rate is $\sim 40M_{\odot} \text{ yr}^{-1}$. This star formation rate is consistent with the luminosities of LBGs. Furthermore, this rate converts only $\sim 2\%$ of the available gas into stars in 10^8 yr , making our assumption of continuous star formation for $\sim 10^8$ years plausible. We also note that in this model, the required star formation rate for a halo of mass M at redshift z scales approximately as

$$\dot{M}_{\star} \approx 40 \frac{M_{\odot}}{\text{yr}} \left(\frac{M_{\text{halo}}}{10^{12}M_{\odot}} \right)^{5/3} \left(\frac{1+z}{4.4} \right)^4, \quad (7)$$

making it easier for ionizing radiation to escape from smaller halos (see Haiman & Rees 2001 for details).

The model described above is highly idealized, and should be regarded only as a plausibility argument that large escape fractions are possible with an extended gas distribution. These models predict that the photoionized cold gas could be detectable in the Ly α recombination line, as a low surface brightness “fuzz” with $\gtrsim 10^{-18} \text{ erg s}^{-1} \text{ cm}^{-2} \text{ asec}^{-2}$. Deep Ly α imaging of extended regions around the LBGs can therefore furnish a method to test this model (see Haiman & Rees 2001 for a similar discussion in the context of bright quasars).

An alternative scenario is one in which the cold gas resides in clumps with a small covering factor. This could allow most of the ionizing photons to escape along lines of sights traversing only hot, collisionally ionized, medium. However, in a self-gravitating two-phase medium, this explanation requires a minimum cold clump size that exceeds the Jeans mass of the cold phase (Rees 1988). As a result, the postulated large clumps would be unstable to fragmentation, which would tend to increase the covering factor to unity. Nevertheless, the covering factor of cold gas can be decreased by feedback mechanisms. Indeed, Pettini et al. (2001) found evidence for galactic scale outflows (“superwinds” of several hundred km/s) in the spectra of LBGs to be ubiquitous. As noted in Pettini et al. (2001), such superwinds, driven by mechanical energy from supernova and stellar winds, can punch holes through the galactic disk, through which the ionizing radiation can escape.

4. Discussion

To summarize, the accuracy of the present constraints on the baryon fraction from the Ly α forest is limited by our knowledge of the ionizing background. A slight tension does exist between such constraints and the nucleosynthesis value, in that the forest measurements tend to prefer higher values for $\Omega_b h^2$. However, even assuming the largest estimate of the ionizing background, which is dominated by contributions from Lyman-break galaxies as reported by Steidel et al. (2001) (see model 3 in §2.2.1), the nucleosynthesis value is ruled out only at the 3σ level.

We emphasize also that even if the ionizing background is known to high accuracy, substantial uncertainties remain, largely due to the uncertain thermal state of the intergalactic medium (parametrized by T_0 and γ – the temperature at mean density and the equation of state index; see §2.1). Present measurements give a probability distribution of $\Omega_b h^2$ which is well-approximated by a Gaussian:

$$P_*(\Omega_b h^2) = \frac{1}{\sqrt{2\pi}0.0061} \exp[-(\Omega_b h^2 - 0.046)^2/0.0061^2] \quad (8)$$

if J_{HI} is fixed to be unity. We show in eq. (6) how the above probability can be used to obtain the probability distribution for $\Omega_b h^2$, $P(\Omega_b h^2)$, given any distribution for J_{HI} (in the extreme case, a delta function). This will be useful as measurements of J_{HI} improve. We also show in §2.2.1 how the lower bound likelihood can be obtained from a given $P(\Omega_b h^2)$ – this is a more appropriate quantity to consider if only strictly lower limits to the ionizing background are known.

Our results show that future improvements in the Ly α forest constraint on the baryon fraction will have to rely on improvements in measurements of the ionizing background and of the thermal state of the gas. The former can be achieved through a variety of means. Measurements of the ionizing flux from LBG’s extending to the redder population and fainter magnitudes will be useful. Improved measurement of the proximity effect would, in principle, be especially powerful because it measures the sum total background of all sources. However, one main source of uncertainty is the large velocity shifts between different lines which affects estimates of the effect as a function of distance from quasars (see e.g. Scott et al. 2000). In addition, systematic effects due to clustering and peculiar velocities should be taken into account in the translation of absorption line statistics into the background flux – interestingly, Loeb & Eisenstein (1995) argued that these effects generally lead to an *over*-estimate of J_{HI} from standard proximity effect measurements. It is also useful to keep in mind the possibility of measuring J_{HI} from direct imaging of the fluorescent Ly α photons from optically thick systems (Gould & Weinberg 1996). The measurements of Bunker, Marleau & Graham (1998) have already put an *upper* limit on the ionizing background, which at the moment is still quite large (3-sigma upper limit is $j_{\text{HI}} < 2 \times 10^{-21} \text{ erg s}^{-1} \text{ cm}^{-2} \text{ Hz}^{-1} \text{ sr}^{-1}$). Deeper exposure to seek a definite detection would be very useful. As far as the thermal state of the intergalactic medium is concerned, larger sample size is crucial, and several techniques have proven useful for this purpose (e.g. Ricotti, Gnedin & Shull 2000, Bryan et al. 1999, Schaye et al. 1999, McDonald et al. 2001, Choudhury et al. 2000, Zaldarriaga et al. 2000; but see also Meiksin, Bryan & Machacek 2001). We should also mention that a constraint on the baryon density can be obtained from the He II forest as well (e.g. Wadsley, Hogan & Anderson 2000).

Ultimately, as the error-bars on $\Omega_b h^2$ from the forest come down, we will have a very precise test of the gravitational instability model, for the forest in particular as well as for large scale structure in general. A statistically significant disagreement among constraints from the forest, nucleosynthesis and the microwave background would require some basic revision of our model.

The findings of Steidel et al. (2001) regarding the LBG Lyman-continuum deserve further study. Their measurements imply an intrinsically hard stellar spectrum, which seems to require a (perhaps unreasonably) young population of stars (1 million years or so) and/or an initial mass function that is biased towards massive stars. Moreover, the large escape fraction for ionizing photons imply that the cold, optically thick gas in LBG’s is likely distributed quite differently from what has been seen in local galaxies. Possibilities include a model in which the cold gas is spatially extended over the halo, and has not settled into a dense galactic disk; or a disk with large holes punched out by strong stellar winds, as suggested by Pettini et al. (2001).

Finally, it is interesting to note that there are some indications of a similar evolutionary trend in AGN

– a decrease of the escape fraction at lower redshifts. Searches for intrinsic absorption at the Lyman-edge at intermediate redshifts ($0.4 \lesssim z \lesssim 2$) generally turn up only small Lyman edge discontinuities in a small fraction of quasars (see e.g. Koratkar, Kinney & Bohlin 1992, Zheng et al. 1997). On the other hand, there is mounting evidence of strong internal Lyman edge absorption in nearby Seyfert galaxies (Alexander et al. 1999, 2000; Kraemer et al. 1999).

We thank C. Leitherer and M. Pettini for useful discussions, and C. Steidel for electronic data for the observational spectrum in Fig. 3. LH was supported by an Outstanding Junior Investigator Award from DOE. ZH was supported by NASA through the Hubble Fellowship grant HF-01119.01-99A, awarded by the Space Telescope Science Institute, which is operated by the Association of Universities for Research in Astronomy, Inc., for NASA under contract NAS 5-26555.

References

- Alexander, T., Sturm, E., Lutz, D., Sternberg, A., Netzer, H., & Genzel, R. 1999, *ApJ*, 512, 204
Alexander, T., Lutz, D., Sturm, E., Genzel, R., Sternberg, A., & Netzer, H., 2000, *ApJ*, 536, 710
Bi, H. G., Borner, G., & Chu, Y. 1992, *A & A*, 266, 1
Bi, H. & Davidsen, A. F., 1997, *ApJ* **479**, 523
Bond, J. R. & Wadsley, J. W., 1997, *Proc. 12th Kingston Conf., Halifax*, astro-ph 9703125
Bruzual, G., & Charlot, S. 1996, unpublished. The models are available from the anonymous ftp site gemini.tuc.noao.edu.
Bryan, G., Machacek, M., Anninos, P., & Norman, M. L. 1999, *ApJ*, 517, 13
Bunker, A. J., Marleau, F. R., & Graham, J. R. 1998, *AJ*, 116, 2086
Burles, S., Nollett, K. & Turner, M., 2000, submitted to *ApJL*, astro-ph 0010171
Burles, S. & Tytler, D., 1998, *ApJ*, 499, 699
Cen, R., Miralda-Escudé, J., Ostriker, J. P., & Rauch, M., 1994, *ApJ* **437**, L9
Choudhury, T. R., Srianand, R. & Padmanabhan, T. 2000 *MNRAS*, in press, astro-ph 0005252
Choudhury, T. R., Srianand, R. & Padmanabhan, T. 2000 submitted to *ApJ*, astro-ph 0012498
Cooke, A. J., Espey, B., & Carswell, R. F. 1997, *MNRAS*, 284, 552
Croft, R. A. C., Weinberg, D. H., Katz, N., & Hernquist, L., 1998a, *ApJ* **495**, 44
Croft, R. A. C., Weinberg, D. H., Pettini, M., Katz, N., & Hernquist, L., 1999, *ApJ*, 520, 1
de Bernardis, P. et al. 2000, *Nature*, 404, 955
Dove, J. B., & Shull, M. J. 1994, *ApJ*, 430, 222
Dove, J. B., Shull, M. J., & Ferrara, A. 2000, *ApJ*, 531, 846
Draine, B. T., & Lee, H. M. 1984, *ApJ*, 285, 89
Eisenstein, D. & Zaldarriaga, M. 2001, *ApJ*, 546, 2
Fardal, M. A., Giroux, M. L., & Shull, J. M. 1998, *AJ*, 115, 2206
Freedman, W. L. et al. 2001, *ApJ*, in press, astro-ph 0012376
Fukugita, M., Hogan, C. J., & Peebles, P. J. E. 1998, *ApJ*, 503, 518
Giallongo, E., Cristiani, S., D’Odorico, S., Fontana, A., & Savaglio, S. 1996, *ApJ*, 466, 46
Gnedin, N., & Hui, L. 1998, *MNRAS*, 296, 44
Gould, A., & Weinberg, D. H. 1996, *ApJ*, 468, 462
Gunn, J. E., & Peterson, B. A. 1965, *ApJ*, 142, 1633
Haehnelt, M., Madau, P., Kudritzki, R. P., Haardt, F. 2000, submitted to *ApJ*, astro-ph 0010631
Haiman, Z., & Rees, M. J. 2001, *ApJL*, submitted, astro-ph/0101174

- Hanany S., et al. 2000, ApJL, 545, 5
- Hernquist, L., Katz, N., Weinberg, D. H., & Miralda-Escudé, J., 1996, ApJ 457, L51
- Hoopes, C. G., Walterbos, R. A. M., & Rand, R. J. 1999, ApJ, 522, 669
- Hui, L. & Gnedin, N. Y., 1997, MNRAS 292, 27
- Hui, L., Gnedin, N. Y., & Zhang, Y., 1997, ApJ 486, 599
- Jaffe, A. H. et al. 2000, PRL, ...
- Koratkar, A. P., Kinney, A. L., & Bohlin, R. C., 1992, ApJ, 400, 43
- Kraemer, S. B., Turner, T. J., Crenshaw, D. M., & George, I. M., 1999, ApJ, 519, 69
- Lange, A. et al. 2001, PRD, 63, 042001
- Leitherer, C., Ferguson, H. C., Heckman, T. M., & Lowenthal, J. D. 1995, ApJ, 454, L19
- Leitherer, C., Schaerer, D., Goldader, J. D., Delgado, R. M. G., Robert, C., Kune, D. F., de Mello, D. F., Devost, D., Heckman, T. M. 1999, ApJS, 123, 3; electronic data are available at <http://www.stsci.edu/science/starburst99/>
- Loeb, A., & Eisenstein, D. J. 1995, ApJ, 448, 17
- Madau, P. 1995, ApJ, 441, 18
- McDonald, P., Miralda-Escudé, J., Rauch, M., Sargent, W. L. W., Barlow, T. A., Cen, R. 2001, submitted to ApJ, astro-ph 0005553
- McDonald, P., Miralda-Escudé, J., Rauch, M., Sargent, W. L. W., Barlow, T. A., Cen, R., & Ostriker, J. P., 2000, ApJ, 543, 1
- Meiksin, A., Bryan, G., & Machacek, M. 2001, preprint, astro-ph 0102367
- Miralda-Escudé, J., Cen, R., Ostriker, J. P., & Rauch, M., 1996, ApJ 471, 582+
- Mo, H. J., Mao, S., & White, S. D. M. 1999, MNRAS, 304, 175
- Muecket, J. P., Petitjean, P., Kates, R. E., & Riediger, R., 1996, A&A 308, 17
- Najarro, F., Kudritzki, R. P., Cassinelli, J. P., Stahl, O., & Hillier, D. J. 1996, A&A, 306, 892
- Navarro, J. F., Frenk, C. S., & White, S. D. M. 1997, ApJ, 490, 493 [NFW]
- Nusser, A. & Haehnelt, M. 2000, MNRAS, 313, 364
- Osterbrock, D. E. 1989, Astrophysics of Gaseous Nebulae and Active Galactic Nuclei, University Science Books
- Pettini, M., Shapley, A. E., Steidel, C. C., Cuby, J.-G., Dickinson, M., Moorwood, A. F. M., Adelberger, K. L., & Giavalisco, M. 2001, ApJ, submitted, preprint astro-ph/0102456
- Rauch, M. & Haehnelt, M. G. 1995, MNRAS, 275, L76
- Rauch, M., Miralda-Escudé, J., Sargent, W. L. W., Barlow, T. A., Weinberg, D. H., Hernquist, L., Katz, N., Cen, R., & Ostriker, J. P., 1997, ApJ 489, 7
- Rees, M. J. 1988, MNRAS, 231, 91
- Reisenegger, A. & Miralda-Escudé, J., 1995, ApJ 449, 476
- Reynolds, R. J., Tufte, S. L., Kung, D. T., McCullough, P. R., & Heiles, C. R. 1995, ApJ, 448, 715
- Ricotti, M., Gnedin, N. Y., & Shull, J. M. 2000, ApJ, 534, 41
- Schaerer, D., & de Koter, 1997, A&A, 322, 598
- Schaye, J., Theuns, T., Leonard, A., & Efstathiou, G. 1999, MNRAS, 310, 57
- Scott, J., Bechtold, J., Dobrzycki, A., & Kulkarni, V. P. 2000, ApJS, 130, 67
- Steidel, C. C., Pettini, M., & Adelberger, K. L. 2001, ApJ, 546, 665
- Steidel, C. C., & Sargent, W. L. 1987, ApJL, 318, 11
- Tegmark, M., & Zaldarriaga, M. 2000, PRL, 85, 2240
- Theuns, T., Leonard, A., Schaye, J., & Efstathiou, G. 1999, MNRAS, 303L, 58
- Wadsley, J., Hogan, C., & Anderson, S. 2000, Proceedings of Clustering at High Redshift, edited by A. Mazure, O. Le Fevre and V. Le Brun, ASP Conference Series, Vol 200, p. 291

- Weinberg, D. H., Miralda-Escude, J., Hernquist, L., & Katz, N. 1997, *ApJ*, 490, 564
- Wechsler, R. H., Somerville, R. S., Bullock, J. S., Kolatt, T. S., Primack, J. R., Blumenthal, G. R., Dekel, A. 2001, *ApJ*, in press, astro-ph 0011261
- Wood, K., & Loeb, A. 2000, *ApJ*, 545, 86
- Zaldarriaga, M., Hui, L., & Tegmark, M., 2000, submitted to *ApJ*, astro-ph 0011559
- Zaldarriaga, M., Seljak, U., & Hui, L., 2001, *ApJ*, in press, astro-ph 0007101
- Zhang, Y., Anninos, P., & Norman, M. L., 1995, *ApJ* 453, L57
- Zheng, W., Kriss, G. A., Telfer, R. C., Grimes, J. P., & Davidsen, A. F., 1997, *ApJ*, 475, 469

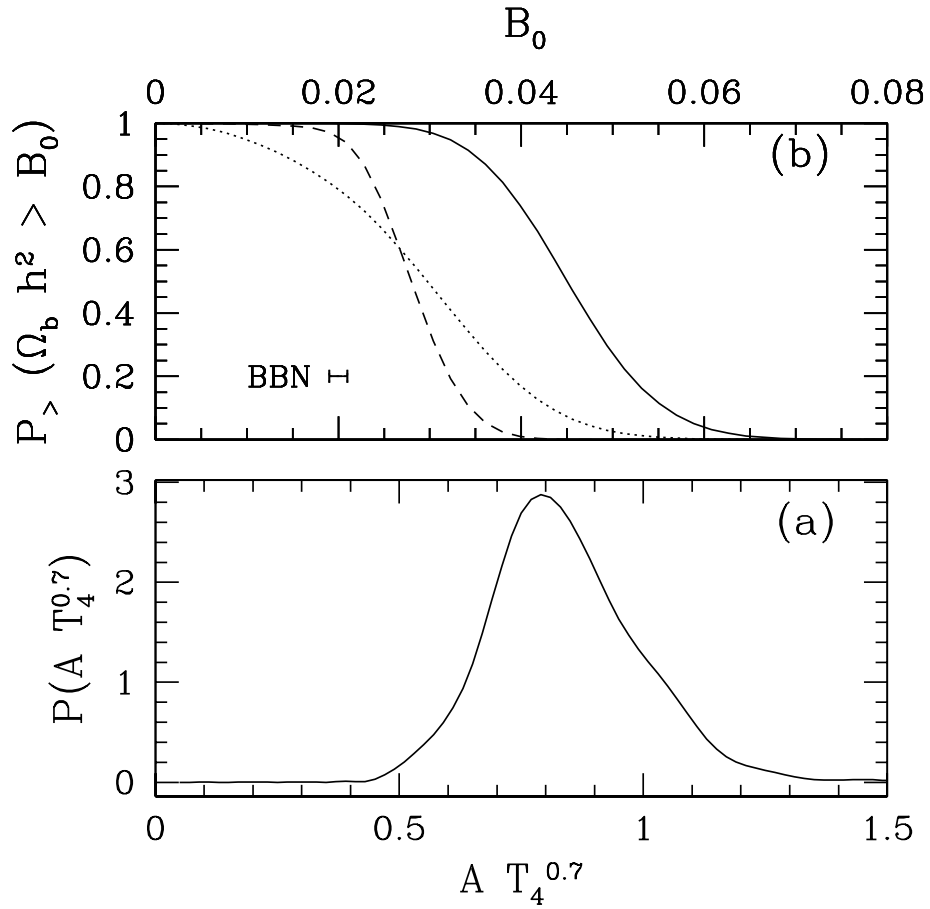


Fig. 1.— (a) Lower panel: likelihood of $A(T_0/10^4 \text{ K})^{0.7}$ at $z = 3$. (b) Upper panel: lower limit to the cumulative probability that $\Omega_b h^2$ is larger than some value B_0 (eq. [4]). Dotted, solid and dashed lines correspond to choices 1, 2 and 3 for $P(J_{\text{HI}})$ respectively (see text). The horizontal bar labeled by BBN gives the nucleosynthesis 68% region.

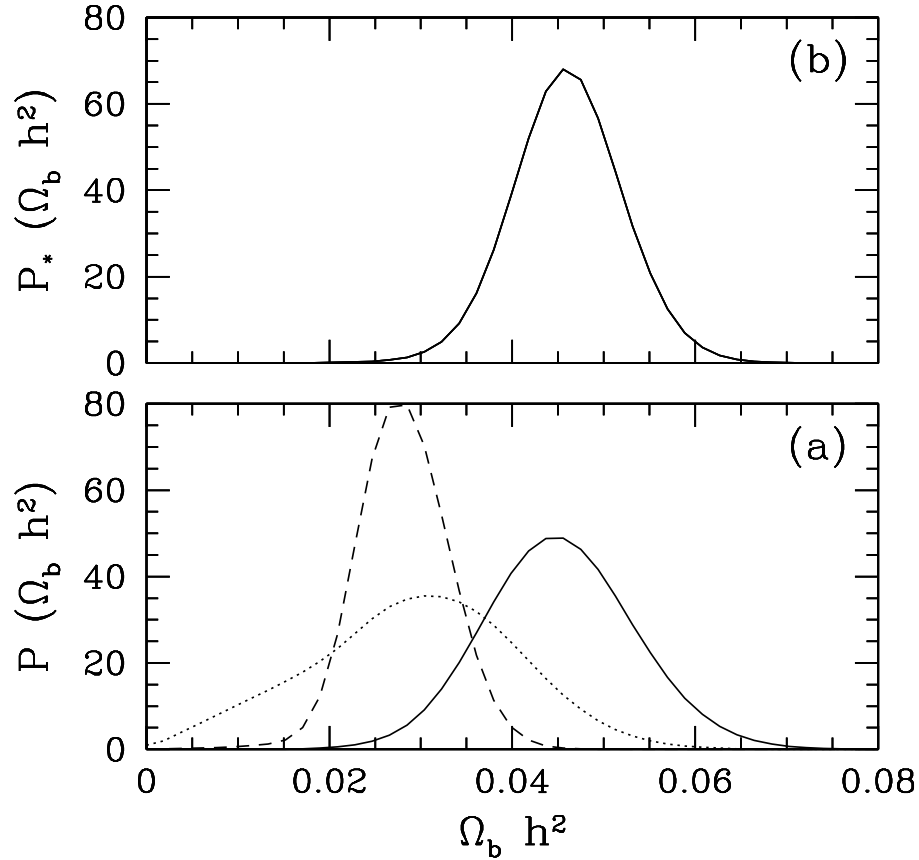


Fig. 2.— (a) Lower panel: the likelihood (differential rather than cumulative distribution) for $\Omega_b h^2$, where dotted, solid and dashed lines correspond to choices 1, 2 and 3 for $P(J_{\text{HI}})$ respectively. These curves derive from differentiation of those in Fig. 1b; see text for details. (b) Upper panel: $P_*(\Omega_b h^2)$, the likelihood for $\Omega_b h^2$ if J_{HI} is fixed to be 1; this is useful for generating the likelihood of $\Omega_b h^2$ for arbitrary distributions of J_{HI} (see eq. [6]). $P_*(\Omega_b h^2)$ is well approximated by a Gaussian of mean = 0.046 and dispersion = 0.0061. For J_{HI} fixed to be some value different from unity, the probability distribution for $\Omega_b h^2$ can be obtained by simply multiplying both the mean and dispersion by $\sqrt{J_{\text{HI}}}$.

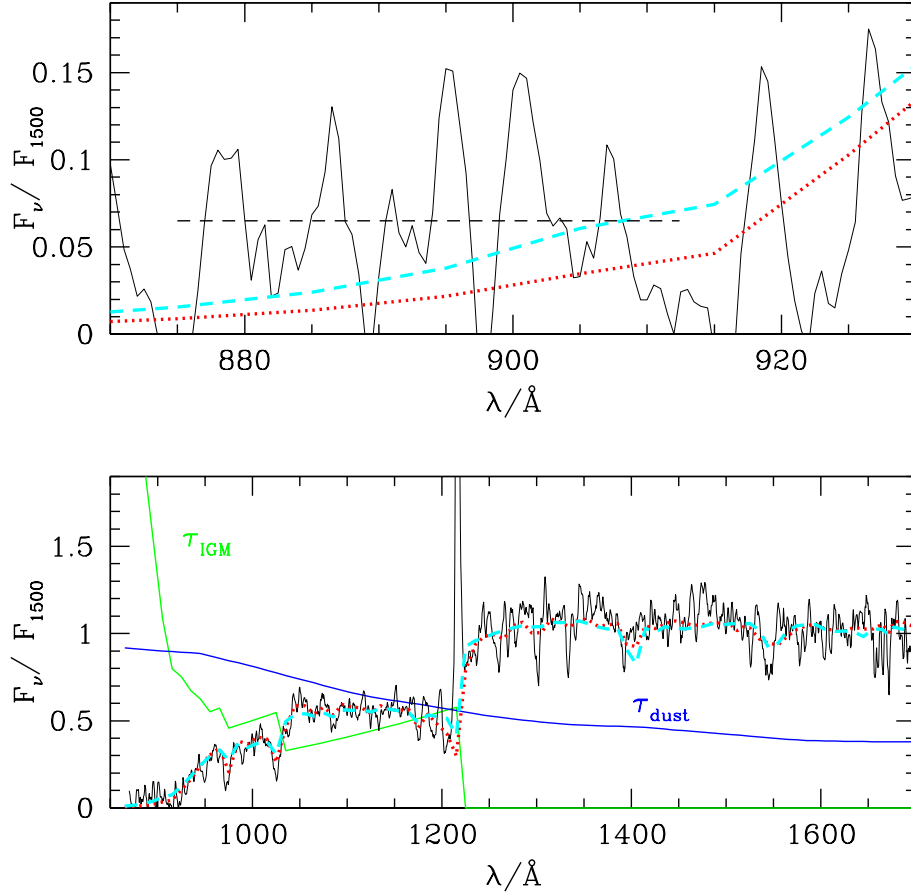


Fig. 3.— Population synthesis spectra, including opacities of dust and neutral hydrogen in the IGM, compared with the observed spectrum of Steidel et al. (2001). The dotted and dashed curves correspond to models of continuous star formation for 10^8 years, and to an instantaneous starburst at 10^6 yr, respectively. The solid curves show the Steidel et al. (2001) composite spectrum. All fluxes are normalized to the flux at the emitted wavelength of 1500\AA . For reference, in the bottom panel, we show the optical depths assumed for the dust and the IGM. In the top panel, the horizontal dashed line shows the mean observed flux in the interval $880\text{\AA} \leq \lambda \leq 910\text{\AA}$.